Fission-Fragment Mass and Charge Distribution for the Moderately Excited U^{236} Compound Nucleus*

J. A. McHugh† and M. C. Michel
Department of Chemistry and Lawrence Radiation Laboratory, University of California, Berkeley, California 94720

(Received 24 January 1968; revised manuscript received 5 April 1968)

The helium-ion-induced fission of Th^{232} (U^{236*}) has been investigated by using high-sensitivity mass-spectrometric techniques. The relative cumulative yields for the majority of isotopes in the mass ranges 83 to 90 and 131 to 153 have been measured. The xenon cumulative yields show no structure at these excitations (20–57 MeV). The independent yields of 15 isotopes produced in the fission of U^{236*} have been measured for various excitation energies ranging from 20 to 57 MeV. In addition, a number of independent and cumulative yields have been measured for the helium-ion-induced fission of U^{235}. The nuclear-charge distribution function was measured directly for one isobaric sequence and indirectly in another; the distribution was found to be Gaussian $y_i \propto \exp[-(Z-Z_p)^2/0.95]$, and independent of the excitation in U^{236*} (to 39 MeV). The empirical Z_p function obtained from our measured independent yields shows none of the trends observed for low-excitation fission of U^{236*} in the 82-neutron-shell region. The total number of neutrons emitted per fission as a function of mass ratio of the fragments was derived from the Z_p function; the neutron yields were found to depend strongly on the asymmetry of the fission mode. Fragment neutron yields were derived from an analysis of the empirical Z_p function and the theoretically predicted Z_p function.

I. INTRODUCTION

SINCE its discovery, the phenomenon of nuclear fission has been investigated by a variety of methods and techniques. One of the basic methods that contributes greatly to the elucidation of the main features of the fission process is the measurement of fission product yields. Two types of yields are measured, independent and cumulative. The independent yield represents a primary product yield after prompt-neutron emission. Yields of this type give information on the division of nuclear charge between the primary fragments. Mass distributions, on the other hand, are obtained from cumulative yields measurements. A number of excellent review articles summarize these and other aspects of nuclear fission.[1–4]

One of the major advancements in fission-yield measurements occurred when mass-spectrometric techniques were introduced. Thode and Graham[5] were the first to utilize this method, and applied it to the measurement of Kr and Xe yields produced from the thermal-neutron fission of U^{235}. In the ensuing years, practically all the major cumulative yield products produced in slow-neutron fission have been investigated in the mass spectrometer.[6] This technique has not been extensively applied to charged-particle–induced fission mainly because of the low product yields ($<10^{-9}$ g) for typical irradiations. Chu,[7] however, showed that with high-sensitivity mass spectrometry and careful chemistry, the relative abundances of a number of elements from charged-particle fission could be determined. Two advantages possessed by mass spectrometry as compared with radiochemistry are readily apparent: (a) Stable-isotope yields can be measured in addition to radioactive species. This is a distinct advantage especially in the measurement of cumulative yields, and of independent yields produced in fission from moderately excited nuclei. (b) In addition to the high precision of this technique, the accuracy compared to radiochemical methods is enhanced because of the elimination of the usual radiochemical problems of decay-curve resolution, knowledge of the decay scheme, and counting corrections.

A large body of data has been obtained relating to the mass and charge distributions for the thermal-neutron–induced fission of U^{235}. However, detailed studies of the energy dependence of various fission features (especially charge distribution) through a wide range of excitation of U^{236*} are scarce. Radiochemical studies of the helium-ion–induced fission of Th^{232} (U^{236*}) were first performed by Newton in 1949, who observed the competition between the symmetric and asymmetric modes in fission.[8] Later Foreman[9] and Davis[10] contributed yield results dealing with the mass distribution, and to a lesser extent with charge distribution.

* This work was performed under the auspices of the U. S. Atomic Energy Commission.

† Present address: Knolls Atomic Power Laboratory, General Electric Co., Schenectady, N. Y. 12301.

[1] R. W. Spencer and G. P. Ford, Ann. Rev. Nucl. Sci. **2**, 399 (1953).

[2] I. Halpern, Ann. Rev. Nucl. Sci. **9**, 245 (1959).

[3] E. K. Hyde, *The Nuclear Properties of the Heavy Elements III, Fission Phenomena* (Prentice-Hall, Inc., Englewood Cliffs, N. J., 1964).

[4] *Proceedings of the Symposium on Physics and Chemistry of Fission* (International Atomic Energy Agency, Salzburg, 1965), Vols. 1 and 2.

[5] H. G. Thode and R. L. Graham, Can. J. Res. **A25**, 1 (1947).

[6] H. Farrar, H. R. Fickel, and R. H. Tomlinson, Can. J. Phys. **40**, 1017 (1962); H. Farrar and R. H. Tomlinson, Nucl. Phys. **34**, 367 (1962).

[7] Yung Yee Chu, University of California Radiation Laboratory Report No. UCRL-8926, 1959 (unpublished).

[8] A. O. Newton, Phys. Rev. **76**, 628 (1949).

[9] Bruce M. Foreman, University of California Radiation Laboratory Report No. UCRL-8223, 1958 (unpublished).

[10] M. E. Davis, Ph.D. thesis, Purdue University, 1963 (unpublished).

The object of our work was to employ the techniques of high-sensitivity mass spectrometry for the accurate measurement of fission yields resulting from Th^{232}-(He^4,f). In particular, major attention was devoted to independent yield measurements so that a detailed analysis of charge distribution could be made. The comparison of experimentally predicted primary yields with a number of postulates[11–20] concerning nuclear-charge division is the general technique for testing the validity of these postulates or prescriptions. However, any interpretation based on experimentally derived primary yields is strongly dependent upon a knowledge of fragment neutron yields. For charged-particle–induced fission, the fragment neutron yields are not known, and thus any ambiguity in the neutron yield will be reflected in the predicted primary yield. Therefore, these experimentally derived yields will not satisfactorily test a proposed mechanism of fission charge distribution. As an alternative, we have taken our primary yield information and directly extracted information concerning neutron yields as a function of mass ratio. From an appropriate charge division mechanism, fragment neutron yields were predicted.

II. EXPERIMENTAL

A detailed description of the experimental procedures can be found elsewhere.[21] Only a brief and general description will be given here.

Target materials for the He^4 bombardments consisted of either 0.001-in. metal foils of Th^{232} and U^{235}, or purified ThO_2. The metal foils were employed for the rare gas, cesium, and rubidium fission yields, whereas purified ThO_2 was employed for the rare-earth fission yield measurements. Purification of the target material for the rare-earth measurements was necessary because the stock thorium contained sufficient natural rare-earth contamination to completely obscure the fission product isotopes produced in a typical irradiation. The ThO_2 was supported for irradiation by hydraulically pressing the oxide into a shallow depression in a copper plate. The ThO_2-copper plate and the foil targets were mounted in conventional microtargets[22] for irradiation. Front cover foils of 0.001-in. aluminum were used in all irradiations. Lower-energy bombardments were achieved by degrading the helium-ion beam with weighed aluminum foils. The energy degradation in aluminum, thorium, and uranium foils was determined from the range energy tables of Williamson and Boujot.[23]

The ultimate sensitivity that can be obtained with the mass spectrometer in the measurement of fission yields is usually limited in practice by natural contamination. If a fission yield of interest is a stable isotope, there exists the possibility that contamination from natural sources can occur. Therefore, the carrier-free target chemistry employed in this work was made as straightforward and simple as possible. The thorium was dissolved and separated from fission products by ion exchange chromatography. A Dowex A-1 column absorbs the Th in $7M$ HNO_3 and passes the fission products of interest. If additional chemistry was unnecessary, the sample was concentrated (by evaporation) and a portion of it was evaporated onto the sample filament of the mass spectrometer. Cation-exchange chemistry[24] was employed to separate the rare-earth fractions. The solid sample analyses were performed with a 12-in.-radius 60°-sector single-direction focusing mass spectrometer of symmetrical design. The ion source used was a double-filament surface ionization source, and the ion detector was an electron multiplier operated in the pulse counting mode.

The rare-gas samples were extracted from the Th and U foils by vacuum fusion in a resistance heated tungsten boat. A hot titanium getter was used to remove reactive gases released in the melting operation. The purified rare-gas fraction was introduced to the gas mass spectrometer and analyzed in the static mode. The gas mass spectrometer is a 6-in.-radius 60°-sector instrument which also employs an electron multiplier ion detector. The ion source is a conventional electron impact source, and the spectrometer is of all metal construction and completely bakeable.

III. TREATMENT OF DATA

A. Cumulative Yields

For the low- and intermediate-energy fission of a heavy nucleus (e.g., U^{236}), the primary fission products are formed with neutron-to-proton ratios greater than

[11] T. J. Kennett and H. G. Thode, Phys. Rev. **103**, 323 (1956).
[12] E. P. Steinberg and L. E. Glendenin, in *Proceedings of the Second United Nations International Conference on the Peaceful Uses of Atomic Energy, Geneva, 1955* (United Nations, New York, 1956), Vol. 7, p. 3.
[13] A. C. Wahl, R. L. Ferguson, D. R. Nethaway, D. E. Troutner, and K. Wolfsberg, Phys. Rev. **126**, 1112 (1962).
[14] L. E. Glendenin, C. D. Coryell, and R. R. Edwards, in *The National Nuclear Energy Series* (McGraw-Hill Book Co., New York, 1951), Vol. 9, Div. IV, p. 489.
[15] A. C. Pappas, MIT Technical Report No. 63 (AECU–No. 2806), 1953 (unpublished).
[16] A. C. Pappas, in *Proceedings of the Second United Nations International Conference on the Peaceful Uses of Atomic Energy Geneva, 1955* (United Nations, New York, 1956), Vol. 7, pp. 19 to 26.
[17] W. E. Grummitt and G. W. Milton, Chalk River Research Report No. CRC-694 (AECL–No. 453), 1957 (unpublished).
[18] A. C. Wahl, J. Inorg. Nucl. Chem. **6**, 263 (1958).
[19] C. D. Coryell, M. Kaplan, and R. D. Fink, Can. J. Chem. **39**, 646 (1961).
[20] H. M. Blann, University of California Radiation Laboratory Report No. UCRL-9190, 1960 (unpublished).
[21] J. A. McHugh, University of California Radiation Laboratory Report No. UCRL-10673, 1963 (unpublished).
[22] S. E. Ritsema, University of California Radiation Laboratory Report No. UCRL-3266, 1956, p. 7 (unpublished).
[23] C. Williamson and J. P. Boujot, Tables of Range and Rate of Energy Loss of Charged Particles of Energy 0.5 to 150 MeV, Centre d'Etudes Nucleaires de Saclay, CEA-2189, 1962 (unpublished).
[24] P. C. Stevenson and W. E. Nervik, U. S. At. Energy Comm. NAS-NS 3020 (1961).

that of the stable nuclei of identical mass. The primary products, therefore, progress up isobaric chains by a series of negatron decays until a long-lived or stable isotope, representing the end product of the fission chain, is reached. The relative yields of the respective fission chains can then be derived from a mass-spectrometric relative-abundance measurement of the chain end products. Fundamentally, this is how the relative chain yields were determined; however, the raw-data treatment requires further discussion because of certain corrections involved.

The analyses of the unspiked samples result in a series of partial yield-mass curves due to the different elements. The normalization of these curves was obtained from the spiked sample. In other words, one atom yield per element was determined from the unspiked and spiked ratios, and from the amount of spike added. In some cases it is possible to normalize the relative yields of adjacent elements through the measurement of a yield they have in common. The mass-144 chain can be measured both in Ce and in Nd since Ce^{144} has an appreciable half-life (285 days), thereby permitting the Ce and Nd relative yields to be normalized without isotope dilution. The Ba^{138} cumulative yield was related to the Cs yields in this manner by measurement of Cs^{136} yield both in Cs and in Ba.

In addition to the rare-earth measurements, relative chain yields were obtained for Kr, Xe, Cs, and Ba isotopes. The Xe and Cs yields could be normalized by measurement of the 133 chain yield in both Xe and Cs; however, this was not done here since all of our targets were allowed to "cool" for a period long compared with the 5-day Xe^{133}. The Cs and Xe yields were normalized by assuming that the Cs^{133} and Cs^{135} yields were consistent with the curve for the Xe yields. We can justify this normalization on the assumption that higher excitation fission has a smoothing effect on possible structure in the yields. This is in agreement with our rare-earth results in that the graphically normalized partial curves agree with the isotopic dilution normalization within the spiking accuracy.

A yield-mass curve was obtained for the 131- to 154-mass region by normalizing our 131-to-138 and 142-to-154 curves through the use of radiochemical yields.[9,10] A rare-earth cross section was chosen from the best fit of the radiochemical yield-mass results to our rare-earth curves, and used along with a similarly obtained cross section from the Xe region as a basis for normalization. The accuracy of such a normalization is not expected to be as high as the mass-spectrometric precision of the relative yields; however, it is hoped to be better than 10% since we used several radiochemical cross sections which best fit our relative yields.

In some instances, the measured yield did not represent the total chain yield. The remainder of the chain is located in isotopes of higher Z. To obtain the correct yield, one could measure and add yields of the higher-Z isotopes, or apply a correction to the partial yield based on the charge distribution in that isobaric sequence. Both methods were employed; for example, the Sm^{150} and Nd^{150} yields were summed to obtain the 150 total chain yield; whereas, the Cs^{137} cumulative yield (a cumulative yield represents the sum of all independent yields preceding and including the given isotope) was corrected by using the charge-distribution function measured in this work to estimate the fraction of the chain beyond Cs.

B. Shielded Isotopes

The yields of isotopes that are shielded by stable or long-lived isotopes from the β^- decay chains represent independently formed fission products. Shielded-isotope measurements comprise most of the unambiguous results on independent fission yields; but since these isotopes lie so close to β stability, lower-energy fission measurements were hampered by their extremely low yields. It is possible at higher excitations to make accurate mass-spectrometric measurements on these shielded isotopes because they now contain an appreciable fraction of the total chain yield.

The Cs^{136}, Cs^{134}, and Cs^{132} independent yields were measured relative to the Cs^{137} cumulative yield. From the previously determined relative chain yields of Xe and Cs, one can obtain fractional chain yields for these isotopes. The independent yields of I^{130}, I^{128}, and I^{126} were obtained through measurement of their stable daughters—Xe^{130}, Xe^{128}, and Xe^{126}—relative to the Xe^{131} chain yield. The contribution of the daughter to the yield is in most cases very small, and an accurate correction can be made by using the charge-distribution function determined in this work. The yield of Xe^{129} which is shielded by the 10^7-yr I^{129} was also measured in the same run. Fractional chain yields for these isotopes, likewise, result from a knowledge of the relative chain yields in this region. However, in this case we must extrapolate our relative yield-mass curve to lighter mass. This was accomplished by a smooth extrapolation based on analysis of radiochemical data in this region.[9,10] The accuracy of such an extrapolation is expected to be better than 5%. The independent yields of Br^{82} and Br^{80} were measured in their Kr daughters relative to the Kr^{84} chain. The necessary relative chain yields for the 82 and 80 chains were derived from an extrapolation of our Kr chain measurements based on a reflection of the complementary rare-earth relative yields. The Br^{80}, I^{126}, and I^{128} exhibit branched decay between β^+, electron capture, and β^- modes. Branching ratios from Strominger *et al.*[25] were used to correct the observed yields. The Pm^{150} fractional chain yield was measured in its stable daughter Sm^{150}.

[25] D. Strominger, J. M. Hollander, and G. T. Seaborg, Rev. Mod. Phys. **30**, 585 (1958).

The independent yield of Rb^{86} was measured. However, in this measurement natural Rb contributed appreciably to the mass-85 and mass-87 fission yields. In order to obtain the yield of Rb^{86} relative to the Rb^{87} chain yield, an assumption concerning magnitude of natural contamination had to be made. Since Rb^{85} is the major natural isotope and is a partial chain yield ($\sim 70\%$) because of hold-up in Kr^{85}, it was assumed to be all natural. This results in an error such that the Rb^{86} fractional chain yield is an upper limit. The relative chain yields at these mass positions were determined by a method identical to that in the previous bromine discussion.

C. Decay Equation for the Mass-135 Chain

In order to obtain direct information concerning the charge-distribution shape, fractional chain yields for two or more members of a fission product chain are required. By observing the growth rate of the long-lived Cs^{135} from the isobaric chain, it is possible to calculate from the equations of radioactive transformation the major primary yields in this chain. The fractional yields of Cs^{135} and Xe^{135}, and fractional cumulative yield of I^{135}, have been measured by this method.

The observation of the growth was made by chemically separating the Cs^{135} from its precursors at a specified time, then measuring the accumulated Cs^{135} relative to Cs^{137} (Cs^{137} precursors have completely decayed prior to Cs separations). The Xe and I fission products are removed in the process of dissolving the Th, and converting it to a solution $7M$ in HNO_3. The anion column which is used immediately following the dissolution to separate Cs from Th will retain any iodine that may not have been removed in the preceding process. A tracer check was performed with carrier-free I^{131} to confirm that the iodine is effectively removed prior to the column separation. Measurements of the Cs^{135}/Cs^{137} ratio were made for three decay times: approximately 1 h, 13 h, and 8 days after irradiation.

Upon consideration of the 135 decay chain, where x, y, and z are the independent production rates of I, Xe, and Cs, respectively, and f is the fraction of the independent yield which populates the 15-min Xe^{135} isomer, we can drive an expression for the observed

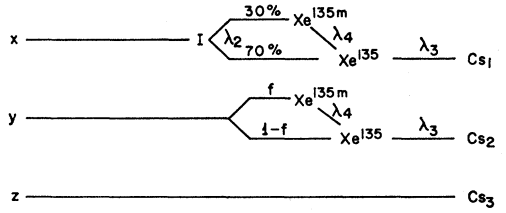

FIG. 1. Decay chain for mass 135. The quantities x, y, and z are the independent production rates of I, Xe, and Cs, respectively, and f is the fraction of the independent yield that populates the 15-min Xe^{135} isomer.

Cs^{135} yield as a function of the production rates, time from beginning of irradiation to separation, t, and the length of irradiation, T. See Fig. 1 and Eqs. (1)–(3):

$$\begin{aligned}Cs_1=0.7x\Big\{&T-\frac{\lambda_2 e^{-\lambda_3 t}}{\lambda_3(\lambda_2-\lambda_3)}[e^{\lambda_3 T}-1]\\&+\frac{\lambda_3 e^{-\lambda_2 t}}{\lambda_2(\lambda_2-\lambda_3)}[e^{\lambda_2 T}-1]\Big\}\\&+0.3x\Big\{T-\frac{\lambda_2\lambda_3 e^{-\lambda_4 t}}{\lambda_4(\lambda_2-\lambda_4)(\lambda_3-\lambda_4)}[e^{\lambda_4 T}-1]\\&-\frac{\lambda_4\lambda_3 e^{-\lambda_2 t}}{\lambda_2(\lambda_2-\lambda_4)(\lambda_2-\lambda_3)}[e^{\lambda_2 T}-1]\\&+\frac{\lambda_2\lambda_4 e^{-\lambda_3 t}}{\lambda_3(\lambda_2-\lambda_3)(\lambda_3-\lambda_4)}[e^{\lambda_3 T}-1]\Big\},\end{aligned}\tag{1}$$

$$\begin{aligned}Cs_2=fy\Big\{&T-\frac{e^{-\lambda_3 t}}{\lambda_3}[e^{\lambda_3 T}-1]\Big\}\\&+(1-f)y\Big\{T-\frac{\lambda_4 e^{-\lambda_3 t}}{\lambda_3(\lambda_4-\lambda_3)}[e^{\lambda_3 T}-1]\\&+\frac{\lambda_3 e^{-\lambda_4 t}}{\lambda_4(\lambda_4-\lambda_3)}[e^{\lambda_4 T}-1]\Big\},\end{aligned}\tag{2}$$

$$Cs_3=zT.\tag{3}$$

Since

$$\frac{Cs^{135}(t)}{Cs^{137}}\propto\frac{Cs_1(x,t,T)+Cs_2(y,t,T)+Cs_3(z,t,T)}{T},$$

three measurements of Cs^{135}/Cs^{137} for t_1, t_2, and t_3 completely specify the production rates x, y, and z, which are directly related to fractional chain yields. The Cs^{135} fractional chain yield is given by $x/(x+y+z)$; similar expressions give the fractional yields of Xe^{135} and I^{135}. If the Ba^{135} fractional chain yield is appreciable, it must be considered. In other words, the above fractional-chain-yield expressions must be multiplied by the fraction of the total chain present. In our measurements the Ba^{135} yield was negligible.

IV. RESULTS

Table I gives the relative cumulative yields of Ce, Nd, and Sm isotopes for the fission of U^{236*} ($Th^{232}+He^4$) at 39.3-MeV excitation. The observed relative yields of each element have been listed separately. These observed yields have been corrected wherever necessary for decay of the isotope under consideration, or for incomplete decay of a precursor by using the first choice of half-lives given by Strominger *et al.*[25] The yields have been normalized to the mass-143 yield (taken as unity)

TABLE I. Relative cumulative yields of Ce, Nd, and Sm isotopes in U^{236*} fission at 39.3-MeV excitation.

Mass No.	Observed relative yields			Normalized relative yields
	Ce	Nd	Sm	
142	1.000			1.115±0.025
143		1.000		1.000±0.006
144	0.740[a]	0.825[a]		0.825±0.016
145		0.713		0.713±0.011
146		0.574		0.574±0.010
147			1.490[a]	0.426±0.002
148		0.355		0.355±0.009
149			1.000	0.286±0.002
150		0.218		0.224±0.006
151			0.598	0.171±0.005
152			0.441	0.126±0.003
154			0.224	0.064±0.0025

[a] Corrected for decay (see text).

by methods previously described, and listed in the last column of Table I.

For convenience, we have presented all $Th^{232}+He^4$ results in terms of the excitation of the U^{236*} compound nucleus. Comparisons of results from neutron-induced fission of U^{235} (U^{236*}) and the He^4-induced fission of Th^{232} are thus based on the excitation in the U^{236*} system. The He^4 bombarding energy required to produce a particular U^{236*} excitation E^* (MeV) is given by E_{He^4} (MeV)$\approx E^*+5.0$ within the energy range used in these experiments.

The relative cumulative yields of Kr, Sr, Xe, Cs, and Ba isotopes are tabulated in Table II. The Kr^{85} yield in the "observed" column represents only the yield of the 10-yr isomer since the shorter-lived 4-h isomer had completely decayed before the fission gases were extracted and analyzed. The Kr and Xe yields were normalized from a knowledge of the relative sensitivity of the mass spectrometer for these isotopes. The sensitivity was determined from an analysis of the rare-gas fraction from thermal-neutron fission of U^{235} where the relative fission yields of Kr and Xe are known.[6]

TABLE II. Relative cumulative yields of Kr, Sr, Xe, Cs, and Ba isotopes in U^{236*} fission at 39.3-MeV excitation.

Mass No.	Observed relative yields				Corrected and normalized[a] relative yields	
	Kr	Sr				
83	0.778				(0.778)	0.256
84	1.000				(1.000)	0.330
85	0.309				(1.215)	0.400[b]
86	1.414				(1.416)	0.467
88		1.00			(1.82)	0.600
90		1.24			(2.25)	0.742
	Xe	Cs	Ba			
131	1.000					1.000
132	1.021					1.022
133		1.006				1.033
134	1.012					1.043
135		1.000				1.033
136	0.767		1.00[c]			1.010
137		0.812				0.862
138			3.14			0.764

[a] Corrected for yields in the higher-Z members of the same chain; column in parentheses is the normalized Kr and Sr data, whereas the last column contains the yields of all elements listed relative to Xe^{131}.

[b] Relative mass yield for the 85 chain obtained from a smooth curve fitted to the 83-, 84-, and 86-mass yields.

[c] The Ba^{136} yield contains only independent yields of Cs^{136} and Ba^{136} since it is shielded by Xe. The measured yield represents 0.241 of the total 136 chain yield (determined from measured fractional chain yield of Cs^{136}).

Table III contains the relative cumulative yields of Kr, Xe, and Cs produced in the He^4 induced fission of Th^{232} and U^{235}. All corrections for residual yields in the higher-Z members of an isobaric sequence have been based on the Gaussian charge distribution measured in this work. All errors in relative cumulative yield measurements are of the order of, or less than, 1% unless otherwise designated. If errors are designated, they are derived from the standard deviation in the results of a large number of mass spectra.

The fractional chain yields of Cs^{135} and Xe^{125}, and the fractional cumulative yield of I^{135}, are listed in Table IV for fission at excitation energies of 39.3, 26.8, 23, and ~17 MeV in the U^{236*} compound nucleus. The yields of Cs^{135} relative to Cs^{137} for three separate decay periods t (decay period measured from beginning of irradiation) and the duration T of each irradiation have also been tabulated for each energy in Table I. It is from these data and the transformation equations derived earlier that the above listed fractional yields are calculated.

Table V gives the fractional chain yields of a number of shielded isotopes produced from the He^4-induced fission of Th^{232} (U^{236*}) for a variety of excitation energies. The independent yields have been measured relative to a neighboring chain yield in the same element. The column designated "measured as" lists for each isotope the manner in which it was measured, and the cumulative yield to which it was compared. The mass-spectrometrically measured ratios are listed under the "observed yield" heading (Cs^{136}, Rb^{86}, and Cs^{132} yields include small decay corrections). The observed independent yields were converted to fractional chain yields by dividing by the relative total chain yield for that particular mass chain. Because a number of independent yields were measured in stable daughters, corrections for the small independent yields of the daughter had to be applied to the observed fractional chain yields. These corrections were determined from the charge-distribution function measured in this work. In addition, the yields measured in the Br^{80}, I^{126}, and I^{128} daughters required correction for branched decay in the parent. The last column of Table V lists the corrected fractional chain yields along with an explanation of each correction. Those values given in parentheses represent upper limits.

Table VI gives fractional chain yields for the He^4-induced fission of U^{235} at 43.6-, 38.0-, 33.8-, and 28.0-MeV He^4. An additional correction is required for these results because of the isotopic composition of the target

TABLE III. Relative cumulative yields of Kr, Xe, and Cs for the He^4-induced fission of Th^{232} and U^{235}.[a]

Mass	83/84	85/84[b]	86/84	132/131	134/131	135/131	136/131	137/131
Excitation energy (MeV)				$Th^{232}+He^4 \rightarrow U^{236*}$				
57.0	0.800	0.343	1.361	0.978	0.922		0.828	
43.5	0.788	0.312	1.384	0.998	1.007		0.957	
37.1	0.772	0.303	1.417	1.027	1.074		1.061	
35.1	0.770	0.295	1.426	1.034	1.074		1.063	
33.1	0.760	0.291	1.434	1.046	1.095		1.104	
31.1	0.749	0.291	1.437	1.057	1.120	1.140	1.156	0.986
28.7	0.737	0.285	1.445	1.064	1.134	1.148	1.161	0.998
23.1	0.710	0.275	1.481	1.106	1.220	1.233	1.243	1.084
21.0	0.691	0.269	1.505	1.136	1.271	1.264	1.246	1.168
He^4 energy (MeV)				$U^{235}+He^4 \rightarrow Pu^{239*}$				
43.6	0.823	0.380	1.394	1.007	0.973		0.884	
38.0	0.814	0.361	1.403	1.016	1.018		0.922	
33.8	0.806	0.341	1.415	1.018	1.037		1.162	
28.0	0.787	0.320	1.436	1.046	1.109		1.150	

[a] The relative mass yields were corrected for yields in the higher-Z members of the same chain when required. The mass 83, 84, 85, and 86 yields were measured in Kr; the mass 131, 132, 134, and 136 yields in Xe; the mass 135 and 137 yields in Cs—the 135 and 137 yields are normalized to Xe^{131} (see text).
[b] The relative mass yield for the 85 chain represents only the Kr^{85} (10 yr) cumulative yield.

material. The foils used in the experiments were 93% U^{235} and 7% U^{238}. Corrections for the contribution of He^4-induced fission of U^{238} to the independent and chain yields of U^{235} were based on the data of Chu.[7]

The errors quoted for the fractional yields are the result of the standard deviation in the measured ratios plus any uncertainty in the relative chain yield used in deriving the fractional chain yield.

V. DISCUSSION

A. Mass Distribution

The yield-mass distribution is still predominantly asymmetric at 39-MeV excitation. A yield-mass curve for U^{236*} ($E^*=39.3$ MeV) is shown in Fig. 2. The curve in the symmetric region was derived from an extrapolation of the higher-mass yield region, and a radiochemically measured valley-to-peak ratio.[10] The ordinate was adjusted so that the total area under the curve integrated to 200%; thus it now represents the approximate fission yield (%). Since there are not enough data in the light-mass region, we cannot determine the number of neutrons emitted as a function of mass ratio by reflection of the fission yields. Davis[10] observed upon folding his radiochemical cumulative yield results for Th^{232}(39-MeV He^4, f) that about five neutrons were emitted per fission. He also noted that this was low compared to what is expected at this excitation. However, these results were based on mass reflections for quite asymmetric fission modes and, therefore, would only yield ν_T for this region. As shown later in this paper, ν_T is dependent on mass ratio, and decreases as the asymmetry of the mode is increased. The value of about five neutrons obtained by Davis[10]

TABLE IV. Fractional chain yields of 135 chain for fission of U^{236*}.

Observed 135/137	$t(h)$	$T(h)$	Cs^{135}	Xe^{136}	I^{135}[a]
		39.3-MeV excitation			
0.1665±0.0031	1.57	0.917			
0.6632±0.0060	13.30	0.917			
1.231 ±0.007	197	0.917	0.098±0.006	0.523±0.010	0.376±0.009
		26.8-MeV excitation			
0.0795±0.0008	1.78	0.883			
0.5174±0.0022	13.07	0.900			
1.169 ±0.010	300	0.900	0.032±0.004	0.381±0.009	0.586±0.012
		23.0-MeV excitation			
0.0560±0.0018	1.77	0.65			
0.5347±0.0051	14.73	0.65			
1.140 ±0.007	350	1.07	0.014±0.004	0.333±0.009	0.653±0.015
		15.0- to 18.0-MeV excitation			
0.0191±0.0025	1.78	0.883			
0.3976±0.0066	13.07	0.900			
1.084 ±0.011	300	0.900	(<0.009)	0.22 ±0.010	0.78 ±0.02

[a] I^{135} is a fractional cumulative yield.

TABLE V. Fractional chain yields for fission of U^{236*}.

Independent yield of	Measured as	Observed yield	Fractional chain yield[a]	Corrected fractional chain yield
		57.0-MeV excitation		
Br^{80}	$Kr^{80}:Kr^{84}$	($\leqslant$0.00096)	($\leqslant$0.0023)	($\leqslant$0.0025)[b]
Br^{82}	$Kr^{82}:Kr^{84}$	0.0260	0.0400	0.0400±0.0026
I^{126}	$Xe^{126}:Xe^{131}$	0.00171	0.00155	0.0039±0.0004[c]
I^{128}	$Xe^{128}:Xe^{131}$	0.0638	0.0602	0.0633±0.0013[d,e]
Xe^{129}	$Xe^{129}:Xe^{131}$	0.00849	0.00816	0.0082±0.0004
I^{130}	$Xe^{130}:Xe^{131}$	0.350	0.343	0.315±0.004[e]
		43.5-MeV excitation		
Br^{82}	$Kr^{82}:Kr^{84}$	0.0120	0.0183	0.0183±0.0015
I^{128}	$Xe^{128}:Xe^{131}$	0.0205	0.0205	0.0219±0.0006[d]
Xe^{129}	$Xe^{129}:Xe^{131}$	0.00289	0.00289	0.0029±0.0003
I^{130}	$Xe^{130}:Xe^{131}$	0.187	0.187	0.180±0.004[e]
		39.3-MeV excitation		
Br^{80}	$Kr^{80}:Kr^{84}$	($\leqslant$0.00026)	($\leqslant$0.00070)	($\leqslant$0.00076)[b]
Kr^{81}	$Kr^{81}:Kr^{84}$	($\ll$0.00014)	($\ll$0.00030)	($\ll$0.00030)
Br^{82}	$Kr^{82}:Kr^{84}$	0.00847	0.0137	0.0137±0.0003
Rb^{86}	$Rb^{86}:Rb^{87}$	0.00230	0.00267	0.00267±0.00022
I^{126}	$Xe^{126}:Xe^{131}$	0.000101	0.000124	0.00028±0.00005[c]
I^{128}	$Xe^{128}:Xe^{131}$	0.0138	0.0155	0.0165±0.0005[d]
Xe^{129}	$Xe^{129}:Xe^{131}$	0.00113	0.00122	0.00122±0.00013
I^{130}	$Xe^{130}:Xe^{131}$	0.148	0.153	0.149±0.002[e]
Cs^{132}	$Cs^{132}:Cs^{137}$	0.00164	0.00137	0.00137±0.00011
Cs^{134}	$Cs^{134}:Cs^{137}$	0.0377	0.0302	0.0302±0.0013
Cs^{136}	$Cs^{136}:Cs^{137}$	0.278	0.230	0.230±0.008
Pm^{150}	$Sm^{150}:Sm^{149}$	0.020	0.025	0.025±0.003
		37.1-MeV excitation		
Br^{82}	$Kr^{82}:Kr^{84}$	0.0073	0.0120	0.0120±0.0006
I^{126}	$Xe^{126}:Xe^{131}$	0.000065	0.000083	0.00019±0.00006[c]
I^{128}	$Xe^{128}:Xe^{131}$	0.0109	0.0121	0.0129±0.0005[d]
I^{130}	$Xe^{130}:Xe^{131}$	0.129	0.133	0.129±0.002[e]
		35.1-MeV excitation		
Br^{80}	$Kr^{80}:Kr^{84}$	($\leqslant$0.00022)	($\leqslant$0.00058)	($\leqslant$0.00063)[b]
Br^{82}	$Kr^{82}:Kr^{84}$	0.00578	0.00963	0.0096±0.0004
I^{128}	$Xe^{128}:Xe^{131}$	0.00823	0.00968	0.0103±0.0004[d]
Xe^{129}	$Xe^{129}:Xe^{131}$	0.00059	0.00066	0.00066±0.00022
I^{130}	$Xe^{130}:Xe^{131}$	0.112	0.117	0.114±0.002[e]
		33.1-MeV excitation		
Br^{82}	$Kr^{82}:Kr^{84}$	0.00471	0.00805	0.0081±0.0004
I^{126}	$Xe^{126}:Xe^{131}$	($\leqslant$0.000036)	($\leqslant$0.000047)	($\leqslant$0.00011)[c]
I^{128}	$Xe^{128}:Xe^{131}$	0.00633	0.00763	0.0082±0.0004[d]
Xe^{129}	$Xe^{129}:Xe^{131}$	($\leqslant$0.00057)	($\leqslant$0.00064)	($\leqslant$0.00064)
I^{130}	$Xe^{130}:Xe^{131}$	0.0930	0.0979	0.0957±0.0025[e]
		31.1-MeV excitation		
Br^{82}	$Kr^{82}:Kr^{84}$	0.00410	0.00732	0.0073±0.0004
I^{128}	$Xe^{128}:Xe^{131}$	0.00460	0.0058	0.0062±0.0004[d]
I^{130}	$Xe^{130}:Xe^{131}$	0.0773	0.0822	0.0806±0.0019[e]
		28.7-MeV excitation		
Br^{80}	$Kr^{80}:Kr^{84}$	($\leqslant$0.00015)	($\leqslant$0.00050)	($\leqslant$0.00054)
Br^{82}	$Kr^{82}:Kr^{84}$	0.00356	0.00647	0.00647±0.00051
I^{126}	$Xe^{126}:Xe^{131}$	($\leqslant$0.000017)	($\leqslant$0.000024)	($\leqslant$0.000054)[c]
I^{128}	$Xe^{128}:Xe^{131}$	0.00315	0.00420	0.0045±0.0003[d]
I^{130}	$Xe^{130}:Xe^{131}$	0.0624	0.0671	0.0660±0.0018[e]
		26.8-MeV excitation		
Cs^{134}	$Cs^{134}:Cs^{137}$	0.0089	0.0076	0.0076±0.0007
Cs^{136}	$Cs^{136}:Cs^{137}$	0.131	0.111	0.111±0.006
		32.1-MeV excitation		
I^{128}	$Xe^{128}:Xe^{131}$	0.0015	0.0021	0.0023±0.0005[d]
I^{130}	$Xe^{130}:Xe^{131}$	0.0321	0.0357	0.0354±0.0021[e]
Cs^{134}	$Cs^{134}:Cs^{137}$	($\leqslant$0.0078)	($\leqslant$0.0068)	($\leqslant$0.0068)
Cs^{136}	$Cs^{136}:Cs^{137}$	0.0813	0.0713	0.0713±0.0045
		21.0-MeV excitation		
Br^{82}	$Kr^{82}:Kr^{84}$	0.0027	0.0056	0.0056±0.0014
I^{128}	$Xe^{128}:Xe^{131}$	0.0011	0.0018	0.0019±0.0002[d]
I^{130}	$Xe^{130}:Xe^{131}$	0.0235	0.0273	0.0273±0.0030
		15.0- to 18.0-MeV excitation		
Cs^{136}	$Cs^{136}:Cs^{137}$	0.0242	0.0223	0.0223±0.0035

[a] Fractional chain yield is the ratio of the observed independent yield to the total chain yield.
[b] Corrected for branching decay ($0.92\beta^-$).
[c] Corrected for branching decay ($0.44\beta^-$).
[d] Corrected for branching decay ($0.936\beta^-$).
[e] Corrected for independent yield of daughter.

TABLE VI. Fractional chain yields for He^4-induced fission of U^{235}.

Independent yield of	Measured as	Observed yield	Fractional chain yield	Corrected fractional chain yield[a]
		43.6-MeV He^4		
Br^{80}	$Kr^{80}:Kr^{84}$	0.00051	0.00106	0.0012±0.0003[b]
Kr^{81}	$Kr^{81}:Kr^{84}$	(<0.000086)	(<0.00015)	(<0.00015)
Br^{82}	$Kr^{82}:Kr^{84}$	0.0342	0.0495	0.0525±0.0015
I^{126}	$Xe^{126}:Xe^{131}$	0.0025	0.0028	0.0067±0.0005[b]
I^{128}	$Xe^{128}:Xe^{131}$	0.0808	0.0842	0.0938±0.0015[b,c]
Xe^{129}	$Xe^{129}:Xe^{131}$	0.0121	0.0124	0.0132±0.0004
I^{130}	$Xe^{130}:Xe^{131}$	0.396	0.400	0.376±0.006[c]
		38.0-MeV He^4		
Br^{80}	$Kr^{80}:Kr^{84}$	(≤0.00031)	(≤0.00068)	(≤0.00074)[b]
Br^{82}	$Kr^{82}:Kr^{84}$	0.0258	0.0385	0.0410±0.0016
I^{126}	$Xe^{126}:Xe^{131}$	0.00146	0.00168	0.0041±0.0004[b]
I^{128}	$Xe^{128}:Xe^{131}$	0.0573	0.0616	0.0689±0.0018[b,c]
Xe^{129}	$Xe^{129}:Xe^{131}$	0.0069	0.0071	0.0075±0.0003
I^{130}	$Xe^{130}:Xe^{131}$	0.326	0.329	0.318±0.006[c]
		33.8-MeV He^4		
Br^{82}	$Kr^{82}:Kr^{84}$	0.0180	0.0277	0.0295±0.0015
I^{126}	$Xe^{126}:Xe^{131}$	0.000664	0.00087	0.0021±0.0002[b]
I^{128}	$Xe^{128}:Xe^{131}$	0.0334	0.0371	0.0421±0.0014[b,c]
Xe^{129}	$Xe^{129}:Xe^{131}$	0.0036	0.0038	0.0039±0.0002
I^{130}	$Xe^{130}:Xe^{131}$	0.249	0.254	0.251±0.006[c]
Br^{82}	$Kr^{82}:Kr^{84}$	0.0112	0.0181	0.0192±0.0014
I^{126}	$Xe^{126}:Xe^{131}$	0.00020	0.00029	0.00071±0.00015[b]
I^{128}	$Xe^{128}:Xe^{131}$	0.0151	0.0180	0.0204±0.0008[b]
Xe^{129}	$Xe^{129}:Xe^{131}$	0.00154	0.00171	0.0018±0.0001
I^{130}	$Xe^{130}:Xe^{131}$	0.155	0.162	0.164±0.005[c]

[a] All yields corrected for isotopic composition of the target.
[b] Corrected for branching decay.
[c] Corrected for independent yield of daughter.

is in good agreement with the values derived from our results.

The "fine structure" observed for the Xe cumulative yields[26] in the thermal-neutron fission of U^{235} is nonexistent in charged-particle–induced fission (see Fig. 3). One prominent feature of the yield-mass curve is the rapid drop in the mass-137 and -138 yields. The rate at which these yields are decreasing is greater than that rate for the light rare earths. A possible structural

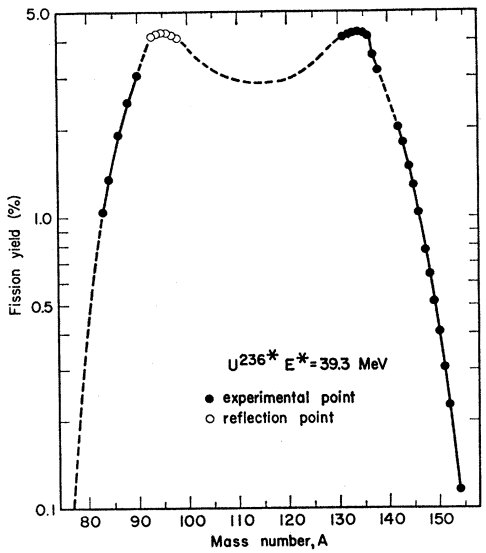

FIG. 2. Yield-mass curve for fission of Th^{232} with 44-MeV He^4.

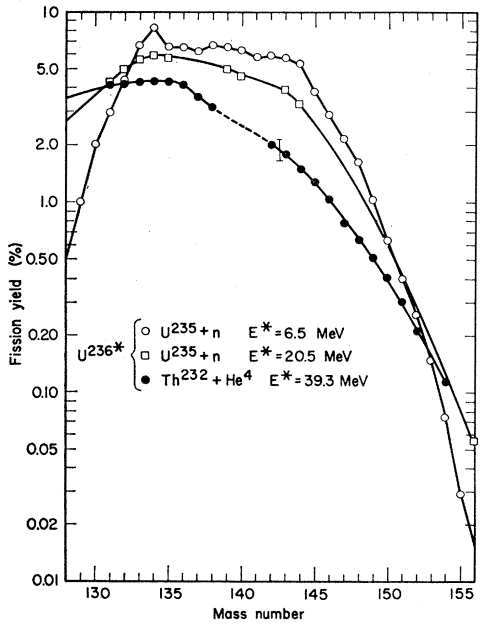

FIG. 3. Heavy wing of the yield-mass curve for U^{235}+thermal neutrons (Ref. 6), U^{235}+14-MeV neutrons [S. Katcoff, Nucleonics 18, 201 (1960)], and Th^{232}+44-MeV He^4. The error bar shown indicates the uncertainty in the normalization of the rare-earth relative yields to the Xe relative yields.

[26] R. K. Wanless and H. G. Thode, Can. J. Phys. 33, 541 (1955).

preference in the fission act, and (or) a variation in neutron emission from the primary fragments could account for this. However, our later results pertaining to charge division suggest shell effects have only a minor influence on the final product distribution.

B. Charge Distribution

1. Charge-Distribution Function

The fractional chain yields for three members of the mass-135 decay chain resulting from the He^4-induced fission of Th^{232} were plotted versus Z. The maximum in the Gaussian curve fitted to the fractional yields for each energy fixes the value of Z_p. The Z_p is the value (not necessarily integral) of the most probable nuclear charge among fission products of the same mass number.

All the 135 chain results are presented as a function of $(Z-Z_p)$ in Fig. 4. The fractional yield data are consistent with a Gaussian curve

$$y_i=(c\pi)^{-1/2}\exp[-(Z-Z_p)^2/c],$$

where y_i is the fractional independent yield of a chain member having atomic number Z, and c is the normalization or width constant of the distribution. The value of c that best fits all energies is 0.95 ± 0.05.

Wahl *et al.*[13] have measured fractional yields for two or more members of several decay chains in the thermal-neutron fission of U^{235}. The value of c obtained from a weighted average of the several chains was 0.94 ± 0.15. Since the same compound nucleus (U^{236*}) was produced in both researches, the above results indicate that a single charge-distribution function is maintained through a wide range of excitations (6.5 to 39 MeV). The charge-distribution curve reported by Blann[27] for $Au+C^{12}$ fission is essentially the same as that found here, within experimental error. These results substantiate the previous conclusions, and, in addition, suggest that there also exists an independence of the charge dispersion with the mass of the fissioning nucleus. Pate *et al.*[28] observed an invariance in the dispersion width at lower energies for the proton-induced fission of Th^{232}.

Swiatecki and Blann[29] have pointed out that a Gaussian charge-distribution function results if the charge fluctuations for a system in thermodynamic equilibrium with harmonic restoring forces can be attributed to statistical and quantum fluctuations. A quantum statistical relationship between the charge-distribution width constant c and the nuclear temperature was derived that is valid for all nuclear temperatures. Their relationship indicates that the width constant should be independent of temperature within the range of excitations that have been reported here (as is observed).

The fractional chain yield of Cs^{136} and the fractional cumulative yield of Xe^{136} for the He^4-induced fission of

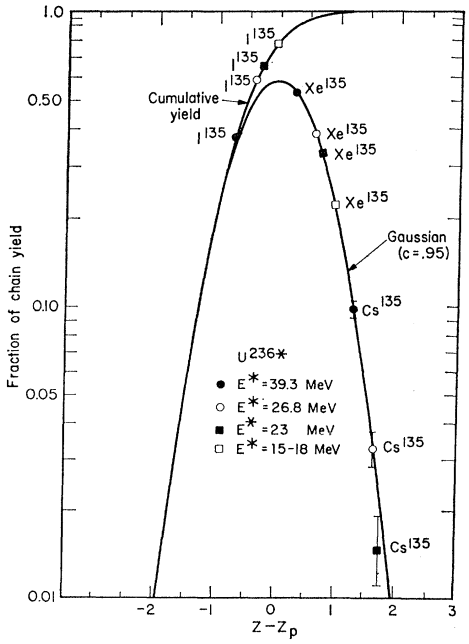

FIG. 4. Gaussian charge-distribution curve that best fit the fractional yield data of the mass-135 chain for all energies.

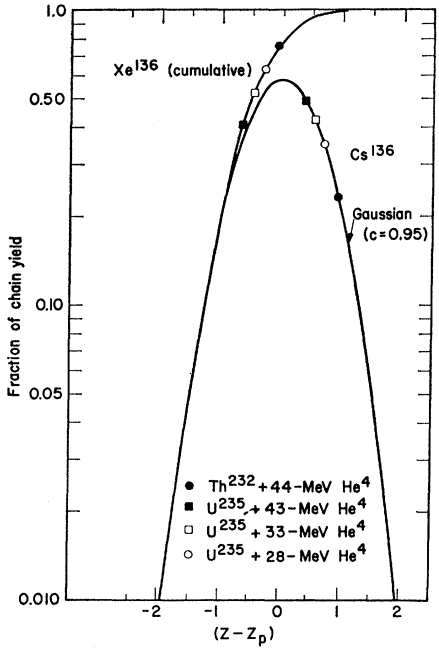

FIG. 5. Fractional yields of Xe^{136} and Cs^{136} as a function of $(Z-Z_p)$. The Xe^{136} cumulative yield is based on the mass-136 chain yield obtained from an extrapolation of lighter-mass Xe chain yields. The Cs^{136} fractional yields for $U^{235}(He^4,f)$ are those of Ref. 38.

[27] H. M. Blann, Phys. Rev. **123**, 1356 (1961).
[28] B. D. Pate, J. S. Foster, and L. Yaffe, Can. J. Chem. **36**, 1705 (1958).
[29] W. J. Swiatecki, Lawrence Radiation Laboratory, Berkeley (private communication).

Th^{232} and U^{235} are fitted best with the identical distribution function found for the 135 isobaric sequence. See Fig. 5.

Due to the close proximity of the 82 neutron shell to the 135 and 136 isobaric chains, one might expect possible perturbations in the primary product yields if nuclear shell structure were influencing the final product distribution. No noticeable deviations from a smooth Gaussian function were observed for the excitations studied. This can be taken to mean that the importance of shell structure has been reduced to a minor level. Colby and Cobble[30] have investigated the independent yields of a few isotopes with one neutron beyond a closed neutron shell. Their conclusions were that these isotopes had abnormally low yields. However, these conclusions were based upon some prescription for predicting Z_p of the particular chain, and thus, as contrasted with our results, were not independent of the assumptions involved in the prescription. If their interpretations were correct, Xe^{137}, which has an appreciable independent yield (~30% of chain yield for some of these energies), would lose a major portion of its yield to Xe^{136}. A change of this order in the Xe^{136} cumulative yield would be easily discernible and was not observed.

2. *Empirical Z_p's and Neutron Emission*

The charge-distribution function for the 135 isobaric chain is uniquely determined from data alone, and is not the result of a correlation of fractional yields from different masses based on a Z_p prediction. Therefore, it is instructive to approach the problem of charge division in a manner similar to Wahl's[18] treatment of thermal-neutron fission of U^{235}. That is, Z_p values for chains in which the fractional yield of only a single member is known may be estimated from the charge-distribution curve previously described, by letting the single fractional yield fix the value of $(Z-Z_p)$, and thus Z_p. An assumption that is automatically injected into the discussion is that the charge dispersions in all mass chains are identical. This appears to be a good assumption at these excitations in view of our results and those of other workers,[13] and indirectly, from the observation of the invariance of the dispersion with excitation energy.

The energy dependence of Z_p for fission resulting from the excited U^{236*} compound nucleus ($Th^{232}+He^4$ and $U^{235}+n$) can now be investigated. Figure 6 is a plot of Z_p versus the excitation in U^{236*}. If an empirical Z_p is known in neutron fission of U^{235} for the masses listed, it is also incorporated in the plot. Above approximately 23-MeV excitation, it can be seen that the Z_p's of the heavy-mass chains vary with energy in similar ways. It is likely that above this energy the fission process has "established" itself. That is to say, the

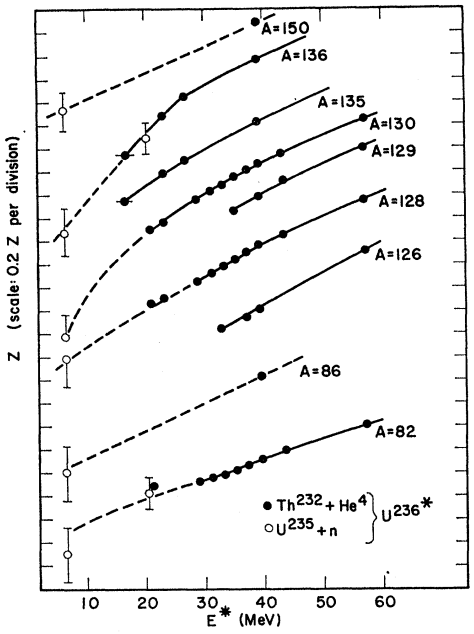

FIG. 6. Empirical Z_p's for the fission of U^{236*} as a function of excitation energy. The $U^{235}(n_{th},f)$ empirical Z_p's are taken from Wahl *et al.* (Ref. 13), except Pm^{150}. The Pm^{150} fractional chain yield of Chu (Ref. 7) has been corrected for Pm^{150} formed by $Sm^{149}(n,\gamma)Pm^{150}$. The $U^{235}(n_{14\ MeV},f)$ empirical Z_p's were derived from data in S. Katcoff, Nucleonics **18**, 201 (1960).

distribution of nuclear charge between the primary fragments is now controlled by a process that is unaltered by additional excitation in the compound nucleus; therefore, the resultant change in Z_p with energy is due only to increased neutron emission at the higher excitations. This smooth and similar variation in Z_p with energy adds support to the assumption of an identical charge dispersion in all mass chains. The fractional chain yields of the separate mass chains are varying over different regions of the charge-distribution curve, yet they still predict the same change in Z_p for a given change in energy. This means that the actual dispersion is identically equal in all isobaric sequences. At lower excitations (below ~23 MeV) a more rapid change of Z_p with energy is observed for the mass-130 and -136 chains. These yields are in the same mass region as the supposedly nuclear-shell–influenced yields produced in the fission of U^{235} by thermal neutrons. It is, therefore, likely that the same factors that depressed the thermal-neutron U^{235} yields are causing the rapid drop of Z_p at these masses as the excitation is lowered.

If we return to the region above E^*~23 MeV for Z_p versus E^*, we can obtain some information concerning the rate of neutron boil-off as a function of excitation energy.

Since

$$(\partial Z_p/\partial E)_A=-(\partial Z_p/\partial A)_E(\partial A/\partial E)_{Z_p}$$

and

$$(\partial A/\partial E)_{Z_p}=-(\partial \nu/\partial E)_{Z_p},$$

[30] L. J. Colby, Jr., and J. W. Cobble, Phys. Rev. **121**, 1410 (1961).

then

$$(\partial\nu/\partial E)_{Z_p}=(\partial Z_p/\partial E)_A/(\partial Z_p/\partial A)_E.$$

The quantity $(\partial Z_p/\partial A)_E$ can be approximated by noting that Z_p closely parallels Z_A, the most stable charge associated with mass number A:

$$(\partial Z_p/\partial A)_E\approx(dZ_A/dA)\approx 0.38$$

or

$$d\nu/dE\approx(\partial Z_p/\partial E)_A/0.38.$$

The average for $(\partial Z_p/\partial E)_A$ in the mass chains closest to symmetry (see Fig. 6, $A=128$ to 138) is 0.026 MeV^{-1}. Since this represents just the change for one fragment and the complementary fragment variation is not known, we approximate the total $d\nu_T/dE$ by taking twice the single fragment change:

$$d\nu_T/dE\approx 2(d\nu/dE)\approx 0.136\ \text{MeV}^{-1}.$$

For a symmetric split, twice the single fragment change should precisely equal $d\nu_T/dE$. A value of $d\nu_T/dE=0.12$ MeV^{-1} was obtained by Leachman[31] from an analysis of the number of neutrons measured experimentally in fission induced by 0- to 14-MeV neutrons. From a correlation of all fission data through ~35-MeV excitation, Powers[32] derived a value of 0.134 MeV^{-1}. Our result can be considered in good agreement with these values. It will be shown later that there is strong evidence the light fragments emit fewer neutrons than the heavy at higher excitations, thus improving the agreement in $d\nu_T/dE$.

Figure 7 shows a plot of Z_p versus He^4 bombarding energy, constructed from results for the He^4-induced fission of U^{235}. Thorium and uranium show the same dependence of Z_p with excitation. In addition, they both show that the Z_p of the light masses (around 82) vary more slowly with E^* than do the Z_p's of the heavy masses. To illustrate this point a bit more dramatically we have plotted in Fig. 8 the fractional chain yield ratio of I^{128}/Br^{82} for a number of energies. We chose I^{128} as the heavy-mass representative because it has approximately the same fractional chain yield as the Br^{82}. If we believe (as was inferred from Fig. 6) that in fission the division of nuclear charge between the primary fragments is independent of excitation at these energies, the only factors that could contribute to the I^{128}/Br^{82} energy dependence are as follows: (1) The charge dispersions in the two mass chains are not identical, and (2) the heavy fragment $d\nu/dE$ is greater than that of the light fragment. Factor (1) is totally inconsistent with our earlier reasoning. In addition, if the distribution were wider for mass 82, which has to be the case if the effect is in the dispersions, the empirical Z_p—predicted from the fractional chain yield and the wider dispersion—would be lowered. The Z_p predicted for this mass on the basis of our Gaussian of $c=0.95$ is already unusually low if the $d\nu/dE$ of the heavy and light fragments are the same. We are left with factor (2) being the more plausible. The $d\nu/dE$ varies, depending on the mass region. It is conceivable that the two listed factors could both contribute to the variation; however, the dominating contributor should be $d\nu/dE$.

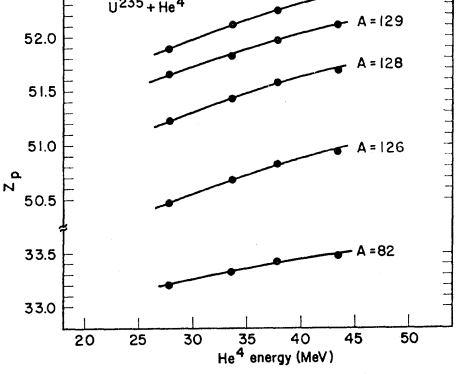

FIG. 7. Empirical Z_p's for U^{235}(He^4,f) as a function of the He^4 bombarding energy.

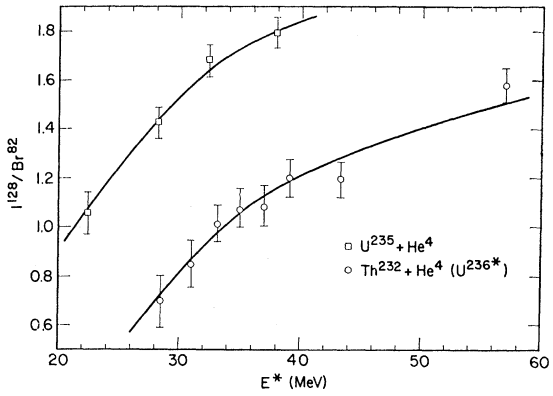

FIG. 8. Fractional chain yield of I^{128} relative to the Br^{82} fractional chain yield as a function of excitation energy for Th^{232}(He^4,f) and U^{235}(He^4,f).

The empirical Z_p's for the He^4-induced fission of Th^{232} and U^{235} are plotted as $Z_p-0.4A$ versus mass number A in Fig. 9. The mass number A is the product after neutron emission. The expanded charge scale $Z_p-0.4A$ was suggested by Coryell[19] so that any structure in the Z_p function would be easily observed.

From Fig. 9 it is shown that a smooth nonwiggly line can be drawn consistent with the data for each case. The resulting lines define the Z_p functions for the two systems. The extrapolation in the intermediate-mass region can be justified by a number of reasons. The accuracy of our data is such that the trends shown for the Z_p's in the light- and heavy-mass regions are un-

[31] R. B. Leachman, in *Proceedings of the Second United Nations International Conference on the Peaceful Uses of Atomic Energy Geneva, 1955* (United Nations, Geneva, 1958), Vol. 15, p. 229.
[32] James A. Powers, Ph.D. thesis, Purdue University, 1962 (unpublished).

questionable (the error bars placed on the data points in Fig. 9 represent the maximum possible error from all sources, assumptions, etc., in each point). This, together with the fact that structure in the Z_p function for the mass-128 to -136 region has disappeared (see Fig. 13) compared to low-energy fission supports the smooth joining of the curves for the two regions. The Z_p function in the intermediate region is in agreement with the energetics involved. One expects from our earlier results for $d\nu_T/dE$ and the results of other workers,[31,32] that at about 40-MeV excitation a total of about seven neutrons should be boiled off per fission. The fact that these are in agreement will be shown next.

It is possible from the Z_p function alone to extract information concerning the total number of neutrons ν_T emitted per fission as a function of the mass split. For a pair of complementary fragments the values $h=(Z_p)_H-0.4A_H$ and $l=(Z_p)_L-0.4A_L$ can be obtained from Fig. 9. If we assume no charged particles emitted at these excitations, then $(Z_p)_L+(Z_p)_H=Z_C$ and $A_L+A_H=A_C-\nu_T$, where Z_C and A_C are the charge

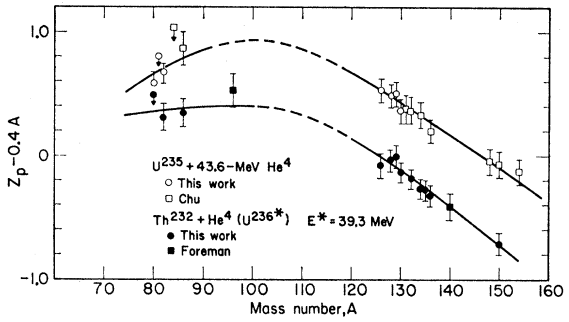

FIG. 9. Empirical Z_p's versus mass number A. Additional experimental data taken from Chu (Ref. 7) and Foreman (Ref. 9).

and mass of the compound nucleus, respectively. From these relationships, it can be shown that for complementary fragments,

$$\nu_T=A_C-2.5Z_C+2.5(h+l). \quad (4)$$

The total number of neutrons ν_T was calculated from Eq. (4) as a function of the mass split by choosing approximately complementary mass fragments (± 1 neutron) for the determination of h and l from Fig. 9. The choice of fragment pairs depends on the total number of neutrons emitted; however, this only affects the derivation of ν_T in second order, and does not change the conclusions to be drawn.

In Fig. 10, ν_T calculated from our Z_p function is plotted versus A_H/A_C. It is readily apparent that there is a strong dependence of ν_T on mass asymmetry. Also shown is the variation of ν_T with mass ratio for the spontaneous fission of Cf^{252} as measured by Stein and Whetstone.[33] The portion of their curve given covers

[33] W. E. Stein and S. L. Whetstone, Jr., Phys. Rev. **110**, 476 (1958).

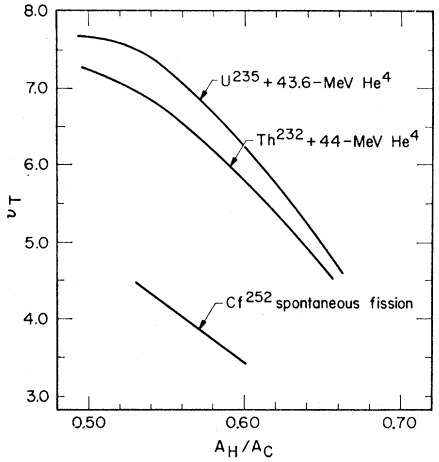

FIG. 10. Total number of neutrons emitted per fission versus the mass fraction A_H/A_C; A_H is product mass after neutron emission. The Cf^{252} data are from the work of Stein and Whetstone (Ref. 33).

the mass ratios containing the great majority of fission events. The variation in ν_T observed for the spontaneous fission of Cf^{252} still appears to be a dominant feature of fission even at higher excitations. The energy partition in fission must be such that the symmetric modes lead to fragments with a greater share of excitation than the asymmetric divisions.

From an analysis of cumulative yield measurements for nearly complementary masses in the deuteron-induced fission of natural uranium, Sugihara *et al.*[34] also observed that fewer neutrons are emitted in modes leading to highly asymmetric products compared with the most probable modes. One of Milton and Fraser's[35] interpretations of the large drop in the total kinetic energy release near symmetry for neutron fission of U^{235}, U^{233}, and Pu^{239} was based on large excitation energies at symmetry. They also pointed out that two types of fission—symmetric fission with highly excited fragments of high kinetic energy—might be associated with the existence of two barriers and two saddle-point shapes as predicted by liquid-drop calculations of Cohen and Swiatecki.[36]

3. *Minimum Potential Energy (MPE) Treatment of Charge Division*

Once the Z_p function has been determined, the next logical step is to seek an explanation or mechanism for the observed division of charge between fragment pairs. The unchanged charge distribution (UCD) hypothesis which enjoyed success for 190-MeV deuteron fission of Bi^{209} (Goeckermann and Perlman)[37] has not received

[34] T. T. Sugihara, P. J. Drevinsky, E. J. Troianello, and J. M. Alexander, Phys. Rev. **108**, 1264 (1957).
[35] J. C. D. Milton and J. S. Fraser, Can. J. Phys. **40**, 1626 (1962).
[36] S. Cohen and W. J. Swiatecki, Ann. Phys. (N. Y.) **19**, 67 (1962).
[37] R. H. Goeckermann and I. Perlman, Phys. Rev. **73**, 1127 (1948).

any substantial support for intermediate-energy fission.[7,38–41] According to this hypothesis, the primary fission fragments have the same neutron-to-proton ratio as in the fissioning nucleus. The UCD hypothesis predicts values of Z_p for the extremely asymmetric mass splits (this is the most sensitive region) that are inconsistent with our results. The charge-to-mass ratios predicted for the heavy fragments are much greater than observed.

Two other postulates which prescribe the manner in which nuclear charge is to be divided in fission are the equal charge displacement (ECD) hypothesis, and the minimum potential energy (MPE) theory. The ECD hypothesis was an empirical suggestion by Glendenin *et al.*[14] which stated that the most probable charges for one fission fragment and for its complementary fragment lie an equal number of charge units away from β stability. The MPE theory proposes that a nucleonic redistribution occurs such that a minimum in the sum of nuclear potential energy and Coulombic repulsion energy is attained. Because the ECD and MPE treatments yield almost similar results for a particular mass formula,[20] we chose the MPE for its theoretical basis—and also for the reason that our results suggested a mechanism that gives the light fragment more than its share of charge, and the heavy fragment less.

The basic ideas embodied in the MPE theory were first proposed by Present.[42] The later MPE formulations of Swiatecki[43] were employed by Blann[20] to describe successfully the charge division for the fission of Au^{197} with 112-MeV C^{12} ions. We will use the MPE treatment, as did Blann, in the framework of the liquid-drop model. Justification for the use of a liquid-drop formulation for fission at moderate excitations lies in the fact that we are now dealing with more highly excited masses where shell influences are probably very minor (our results indicate this to be true). It is, therefore, desirable to describe the nuclear potential energy surface by a smooth function of N and Z. The liquid-drop mass formula of Green[44] has been employed.

The total energy for a fragment pair can be written

$$\mathrm{PE}=M_L+M_H+(Z_HZ_LQ^2)/D, \qquad (5)$$

assuming the configuration at scission can be represented by tangent spheres, where D is the effective separation of the fragment centers; M_L, M_H, Z_L, and Z_H are the mass and charges for the heavy and light fragments; and Q is the unit of elemental charge. Green's mass formula is[44]

$$E=-a_1A+a_2A^{2/3}+a_3Z^2A^{-1/3}+a_4(A-2Z)^2(4A)^{-1}. \qquad (6)$$

The constants given by Green are: $a_1=15.83$, $a_2=17.97$, $a_3=0.718$, and $a_4=94.07$ MeV. Substituting the mass formula into Eq. (5) and minimizing ($\partial\mathrm{PE}/\partial Z_L=0$) with the constraint $Z_L+Z_H=Z_C$, the compound nucleus charge, one obtains for $(Z_p)_L$ (before neutron boil-off from fragments)

$$(Z_p)_L=\frac{Z_C(a_4A_H^{-1}+a_3A_H^{-1/3}-\frac{1}{2}Q^2D^{-1})}{a_3(A_L^{-1/3}+A_H^{-1/3})+a_4(A_H^{-1}+A_L^{-1})-Q^2D}. \qquad (7)$$

Milton[45] gives a similar expression for $(Z_p)_L$, except that his expression contained additional parameters to account for any spheroidal deformation of the fragments at scission. In this work the effective separation of the fragment centers D was chosen so that the $Z_HZ_LQ^2/D$ term of Eq. (5) would yield the correct total kinetic-energy release. The kinetic-energy release is dependent on the mass ratio of the fragments; but because Z_p is rather insensitive to the variations in D needed to describe the kinetic-energy release, an average value for D was taken ($D=18$ F), and held constant in Eq. (7). (The total kinetic-energy release varies by approximately 10% for fission at moderate excitations. This variation amounts to a fluctuation in Z_p of less than 0.05 charge units.)

In order to interpret gainfully the predictions of Eq. (7) as regards the experimentally determined Z_p's, one must know how many neutrons were emitted from the individual primary fragments. Our earlier discussions showed that the total number of neutrons ν_T emitted per fission was dependent on mass asymmetry. This observation, along with some assumption concerning the partition of ν_T between the light and heavy fragments, could be used (as is the usual case in a study of charge distribution) to test the validity of a proposed charge-division prescription by comparing with the experimentally derived Z_p's. However, the assumptions relating to the partition of ν_T at these higher excitations possesses no more strength than the Z_p prescription itself. It is, therefore, proposed that we assume the MPE treatment predicts the exact charge division for the primary fragments, and that from the empirical Z_p's we determine the neutron yields ν_A for the individual fission fragments.

In Figs. 11 and 12 the MPE Z_p functions for 4, 3, 2, and 1 neutron being emitted from the primary fragments are shown along with the empirical Z_p's for the two cases. Also shown are the predicted ν_A's. For Th^{232} +44-MeV He^4 and U^{235}+43.6-MeV He^4 the average fissioning nuclei were taken as U^{235} and $Pu^{238.5}$, respectively. These were chosen so as to be consistent with the branching ratios for neutron emission and fission

[38] N. Souka and M. C. Michel, University of California Radiation Laboratory Report No. UCRL-10555, 1962 (unpublished).
[39] Walter M. Gibson, University of California Radiation Laboratory Report No. UCRL-3493, 1956 (unpublished).
[40] J. M. Alexander and C. D. Coryell, Phys. Rev. **108**, 1274 (1957).
[41] Patrick del Marmol, Ph.D. thesis, Massachusetts Institute of Technology, 1959 (unpublished).
[42] R. D. Present, Phys. Rev. **72**, 7 (1947).
[43] W. J. Swiatecki, Lawrence Radiation Laboratory, Berkeley (private communication to H. M. Blann).
[44] A. E. S. Green, Rev. Mod. Phys. **30**, 569 (1958).
[45] J. C. D. Milton, University of California Radiation Laboratory Report No. UCRL-9883, 1962 (unpublished).

Γ_n/Γ_f, given by Vandenbosch *et al.*[46] and Foreman[9] for these compound systems.

Our results indicate that the sawtooth variation of neutron yields[47,48] with fragment mass observed for spontaneous and thermal-neutron fission disappears in higher-excitation fission. Although the corresponding light-mass regions show a similar variation, the effect in the lightest heavy fragments has been completely "washed out." Britt and Whetstone[49] have reported on the average number of prompt neutrons emitted as a function of fragment mass for the He^4-induced fission of Th^{230} and U^{233}. Their results were derived from a comparison of the mass distributions from double-energy measurements with the mass distributions obtained from double-velocity time-of-flight measurements. The trends they observed are essentially the same as found here (Figs. 11 and 12). In low-energy fission, the minimum in the fragment neutron yield is found in the neighborhood of $N\approx 50$ and $Z\approx 50$ (masses 82 and 128). Terrell[50] suggested that these magic or near-magic fragments have low excitations and consequently emit almost no neutrons, because of greater

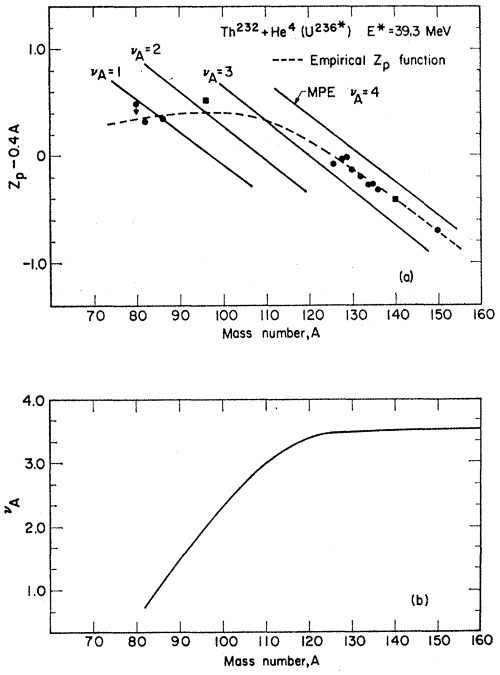

FIG. 11. (a) The most probable charge Z_p in fission of Th^{232} induced by He^4, based on MPE for the emission of 4, 3, 2, and 1 neutron from the primary fragment. (Points are indicated as in Fig. 9.) (b) The fragment neutron yields ν_A needed to fit the empirical Z_p function by MPE. The average fissioning nucleus was taken as U^{235}.

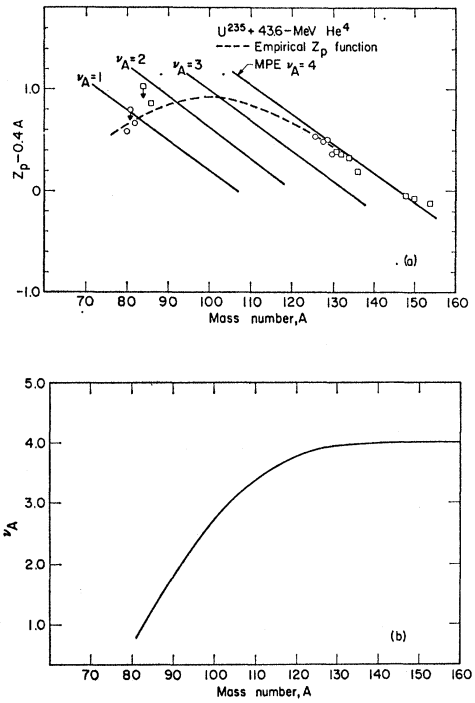

FIG. 12. (a) The most probable charge Z_p in fission of U^{235} induced by He^4, based on MPE for the emission of 4, 3, 2, and 1 neutron from the primary fragment. (Points are indicated as in Fig. 9.) (b) The fragment neutron yields ν_A needed to fit the empirical Z_p function by MPE. The average fissioning nucleus was taken as $Pu^{238.5}$.

rigidity against distortion from near-spherical shapes. This interpretation could be applied to higher-excitation fission in the light-mass region ($N\approx 50$); however, the products near $N\approx 50$ are no longer formed with low excitations. The fact that an appreciable portion of higher-excitation-fission events come from symmetric modes may influence the neutron yields (excitation) more near $Z\approx 50$ than near the $N\approx 50$ region.

Since the primary product neutron yields are known for the thermal-neutron fission of U^{235}, and, in addition, there is a large body of empirical Z_p's for the system, one can meaningfully test the validity of various charge-division prescriptions. Figure 13 shows the empirically determined Z_p's and Z_p functions for $U^{235}(n_{th},f)$ and Th^{232}(44-MeV He^4,f), along with the predictions of UCD (curve A) and MPE (curve B) for $U^{235}(n_{th},f)$. The number of neutrons emitted by a fragment was taken from a straight line fitted to Terrell's[50] corrected experimental data for $U^{235}(n_{th},f)$. In the region near symmetry, the light- and heavy-fragment neutron yields were joined by a smooth curve. The MPE curve is derived by using Green's[44] mass formula and an effective fragment separation D of 18 F. The MPE Z_p function fits the average trend of the empirical Z_p's very well. However, a shell-influenced mass formula would more likely give a better fit to the experimental results for $U^{235}(n_{th},f)$. It is our intent only

[46] R. Vandenbosch, T. D. Thomas, S. E. Vandenbosch, R. A. Glass, and G. T. Seaborg, Phys. Rev. **111**, 1358 (1958).
[47] J. S. Fraser and J. C. D. Milton, Phys. Rev. **93**, 818 (1954).
[48] S. L. Whetstone, Jr., Phys. Rev. **114**, 581 (1959).
[49] H. C. Britt and S. L. Whetstone, Jr., Phys. Rev. **133**, B603 (1964).
[50] J. Terrell, Phys. Rev. **127**, 880 (1962).

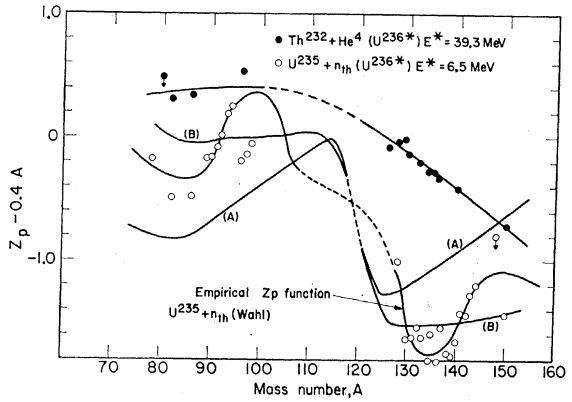

FIG. 13. The empirical Z_p's for U^{236*} are compared; and the comparison is made of empirical Z_p's for $U^{235}(n_{th},f)$ (see Ref. 13) with those predicted by UCD (curve A) and MPE (curve B).

to show that with a knowledge of ν_A and a simple MPE liquid-drop treatment, the average trends in the $U^{235}(n_{th},f)$ Z_p function can be derived. The UCD does not at all predict reasonable Z_p's (as has been observed before).

Coryell *et al.*[19] have proposed a method for deriving the Z_p of any isobaric chain for various types of fission differing in compound nucleus and in excitation energy. Their expression uses the Z_p function for $U^{235}(n_{th},f)$ as a basis function for all computed Z_p's. In their method, the shift in the Z_p function, $\Delta Z_p(A)$ is dependent only on Z_C, A_C, and ν_T, the charge and mass of the compound nucleus, and the total number of neutrons emitted per fission. This method is inapplicable at higher excitations for two reasons: (a) No structure similar to $U^{235}(n_{th},f)$ remains in the Z_p function at higher excitations, and (b) the shift in Z_p because of increased excitation is not the same for all mass chains, as is implied by their prescription.

The foregoing results and discussion of charge distribution strongly suggest the need for a direct experimental determination of fragment neutron yields for fission induced by charged particles. A measurement of this type will remove the major obstacle in the path of answering the question of how nuclear charge is divided in fission at these excitations.

C. Independent Yield Distribution for Isotopes of a Given Z

The relative independent yields of Cs, Xe, and I isotopes provide enough information for deriving a distribution function for the independent yields of isotopes of a given Z. The Cs, Xe, and I independent yields for the highest-energy helium-ion–induced fission of U^{235} and Th^{232} were normalized to the mass-131 total chain yield. Since the yield-mass curves are nearly level in this region, the most probable mass number A_p for a given charge should peak at the same value of cross section for each isotope (Cs, Xe, and I). These conditions—together with the distribution function that best fit all the results—were used to determine the A_p's for each Z.

Figure 14 shows the relative yields y_r plotted versus $A-A_p$. A Gaussian function

$$y_r \propto \exp[-(A-A_p)^2/7] \tag{8}$$

gives the best fit to the data.

It can be shown that this dependence is expected in light of a Gaussian charge dispersion and equal chain yields. The yield for independent formation of a product nuclide is given by

$$y(A,Z)=Y_A(0.95\pi)^{-1/2}\exp[-(Z-Z_p)^2/0.95], \tag{9}$$

where Y_A is the chain yield for mass number A, and the other variables have the usual meanings. Since it is known that the chain yields in this mass region are approximately the same ($Y_A=Y_{A'}$), and $dZ_p/dA=0.365$ (obtained from data in the mass region 126 to 136), or $\Delta Z_p=0.365(A-A')$, the yield $y(A',Z)$ in some other isobaric sequence A' can be derived. Upon setting $\partial y(A',Z)/\partial A'=0$, one obtains A as a function of Z, $(Z_p)_A$, and A_p, where A_p is the mass (not necessarily integral) at which the yields of isotopes of a given Z have a maximum. By substituting for A in $y(A',Z)$, the yield at constant Z becomes

$$y_Z(A')=Y_A(0.95\pi)^{-1/2}\times\exp\{-[0.365(A'-A_p)]^2/0.95\}, \tag{10}$$

or in general

$$y_Z(A)\propto\exp[-(A-A_p)^2/7.1]. \tag{11}$$

The agreement between Eqs. (8) and (11) substantiates the fact that the charge dispersion is a Gaussian of width constant 0.95.

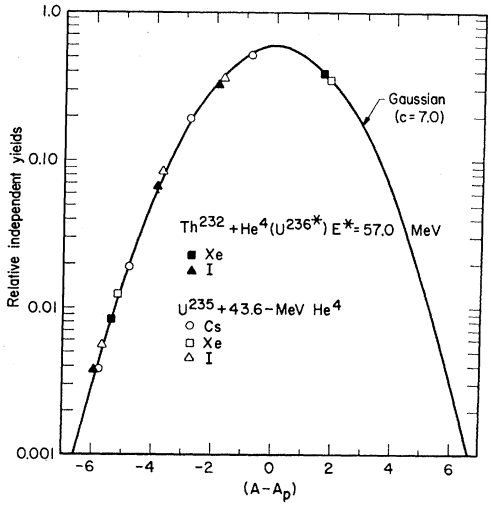

FIG. 14. Relative independent yields of I, Xe, and Cs isotopes versus mass number, $(A-A_p)$. All yields are relative to the Xe^{131} chain yield and the relative Cs independent yields are those of Souka (Ref. 38).

Blann[18] observed that the distribution of independent yields of isotopes for a given Z in the 112-MeV C^{12} fission of Au^{197} could also be described by a Gaussian. However, the distribution width constant ($c=6.0$) was not the same as that of the above distribution ($c=7.0$). Levy and Nethaway,[51] upon an analysis of Blann's results, proposed that symmetric fission may follow a bivariate normal distribution of charge and mass. The Gaussian distribution of mass shown in our work is a consequence of the Gaussian charge dispersion, and the nature of the total mass yields.

VI. SUMMARY

The yield-mass distribution is still predominantly asymmetric at 39-MeV excitation. The fine structure observed for the Xe cumulative yields in thermal-neutron fission of U^{235} is nonexistent in charged-particle–induced fission.

The charge-distribution function was found to be described by a Gaussian function $y_i=(c\pi)^{-1/2}\times\exp[-(Z-Z_p)^2/c]$, where the width constant c was equal to 0.95. The distribution function was found to be independent of excitation energy (to 39 MeV) in the compound nucleus. In addition, no noticeable deviations from a pure Gaussian function were observed for the charge-distribution functions of the mass-135 and -136 isobaric sequences. This, together with the disappearance of fine structure in the Xe cumulative yields, suggests that for excitations above about 23 MeV the influence of nuclear shells on the final fission product distribution has been reduced to a minor level. Further evidence to support this conclusion comes from the empirical Z_p function for U^{236*} at 39-MeV excitation. The function varies smoothly with mass and shows no structure resembling that for $U^{235}(n_{\text{th}},f)$ in the region of the 82 neutron shell. The change in Z_p with energy (dZ_p/dE) derived from our measured energy dependence of the empirical Z_p's is entirely consistent with the energetics of neutron emission, and agrees with experimentally measured $d\nu_T/dE$.

The empirical Z_p function was shown to be useful in extracting information on the mass dependence of the total number of neutrons ν_T emitted in the fission process. An analysis of the Z_p function for the He^4-induced fission of Th^{232} and U^{235} showed ν_T to be strongly dependent on mass asymmetry, and in agreement with the trends observed for the spontaneous fission of Cf^{252}. A greater number of neutrons were found to come from symmetric modes than from asymmetric modes. This suggests that the energy partition in fission is such that symmetric modes receive a greater share of the available excitation energy than do the asymmetric modes.

The neutron yields from the individual fragments can be derived from the empirical Z_p function providing one knows the true charge division. Using the MPE treatment of charge division (for reasons previously given) one finds the ν_A function to be an increasing function of mass up to about the symmetric mass split, and then constant with mass for the heavy region. The trends in the ν_A function for the heavy-mass region in low-energy fission (spontaneous and thermal neutron) have completely disappeared in higher excitation fission.

The distribution function for the independent yields of Cs, Xe, and I was found to be described by a Gaussian function $y_r\propto\exp[-(A-A_p)^2/7]$. The observed dependence was shown to be a consequence of the Gaussian charge dispersion ($c=0.95$) and the nature of the total mass yields. This result reinforces our conclusion that a single charge dispersion function is valid for all mass chains.

ACKNOWLEDGMENTS

We wish to express our appreciation to D. H. Templeton, W. J. Swiatecki, H. P. Robinson, and J. H. Reynolds for helpful discussions. The cooperation of P. McWalters and J. Wood of the cyclotron group is gratefully acknowledged. Thanks are due to F. L. Reynolds and F. Vogelsberg for their aid in various aspects of this work.

[51] H. B. Levy and D. R. Nethaway, University of California Radiation Laboratory Report No. UCRL-6948, 1962 (unpublished).